Stability of the $N=50$ shell gap in the neutron-rich Rb, Br, Se, and Ge isotones

Y. H. Zhang,[1,2] Zs. Podolyàk,[3] G. de Angelis,[1,4] A. Gadea,[1] C. Ur,[5] S. Lunardi,[5] N. Marginean,[1] C. Rusu,[1] R. Schwengner,[6] Th. Kröll,[1] D. R. Napoli,[1] R. Menegazzo,[5] D. Bazzacco,[5] E. Farnea,[5] S. Lenzi,[5] T. Martinez,[1] M. Axiotis,[1] D. Tonev,[1] W. Gelletly,[3] S. Langdown,[3] P. H. Regan,[3] J. J. Valiente Dobon,[3] W. von Oertzen,[4,7] B. Rubio,[8] B. Quintana,[9] N. Medina,[10] R. Broda,[11] D. Bucurescu,[12] M. Ionescu-Bujor,[12] and A. Iordachescu[12]

[1]*Istituto Nazionale di Fisica Nucleare, Laboratori Nazionali di Legnaro, Legnaro, Italy*
[2]*Institute of Modern Physics, CAS, Lanzhou, People's Republic of China*
[3]*Department of Physics, University of Surrey, Guildford, Surrey, United Kingdom*
[4]*Hahn-Meitner-Institut, Berlin, Germany*
[5]*Dipartimento di Fisica dell'Università and Istituto Nazionale di Fisica Nucleare, Sezione di Padova, Padova, Italy*
[6]*Institut für Kern-und Hadronenphysik, Forschungszentrum Rossendorf, Dresden, Germany*
[7]*Freie Universität Berlin, Fachbereich Physik, Berlin, Germany*
[8]*Instituto de Fisica Corpuscular, Valencia, Spain*
[9]*Grupo de Fisica Nuclear, Universidad de Salamanca, Spain*
[10]*Instituto de Fisica, Universidade de Sao Paulo, Sao Paulo, Brazil*
[11]*Institute of Nuclear Physics, Krakow, Poland*
[12]*H. Hulubei National Institute for Physics and Nuclear Engineering, Bucharest, Romania*

The low- and medium-spin states of the $N=50$ neutron-rich, $^{87}_{37}$Rb, $^{85}_{35}$Br, $^{84}_{34}$Se and $^{82}_{32}$Ge isotones have been populated in deep-inelastic processes produced by the interaction of 460 MeV ^{82}Se ions with a ^{192}Os target. The subsequent γ decay has been investigated at the Laboratori Nazionali di Legnaro using the GASP γ-ray detector array. The comparison of the experimentally observed excited states with shell-model calculations performed with and without neutron degrees of freedom has allowed the investigation of the role of the neutron-core breaking excitations and therefore of the $N=50$ shell gap. The inclusion of neutron configurations in the shell-model calculations results in an improved agreement between the experimental and calculated level energies at medium and high spin. These results highlight the considerable contribution of neutron-core particle-hole excitations across the $N=50$ shell gap to the level configurations. The overall agreement of the measured excited states with the shell-model predictions is indicative of the persistence of the $N=50$ shell gap down to $Z=32$.

I. INTRODUCTION

Neutron-rich nuclei close to shell gaps have recently attracted a particular interest triggered by a possible existence of anomalies into the shell structure [1]. Different from proton-rich systems, which are stabilized by the Coulomb barrier, nuclei close to the neutron drip-line are weakly bound and therefore valence neutrons can be very extended spatially. Here, new features like neutron skins or halos have been predicted and major effects are expected due to the pairing interaction and to the influence of the particle continuum.

Neutron-rich nuclei around the shell-model magic numbers $N=20$ and 28 have exhibited properties inconsistent with shell closure [2,3]. Such quenching of the classical shell gaps has also been further corroborated by Hartree-Fock-Bogoliubov (HFB) calculations with SKP force [4] and by using mass predictions from the infinite nuclear matter model [5]. Several experimental results have shown indications of a quenching of the $N=20$ shell in neutron-rich isotopes. The disappearance of the $N=20$ shell gap, predicted by Hartree–Fock calculations [6] and by numerous shell-model studies [7], has, as a consequence an increased collectivity and eventually the stabilization of deformation in light mass, semimagic nuclei. Similarly, it has been suggested, on

the basis of self-consistent mean field calculations, that the major $N=28$ shell gap disappears when approaching $Z=16$. Here the potential energy surfaces become very soft with close lying shallow minima corresponding to different deformations. Experimentally, intermediate-energy Coulomb excitation measurements of the $B(E2;0^+\rightarrow2^+)$ values have shown evidence of collectivity for ^{44}S and ^{46}Ar [8,9]. Recently, in such nuclei indication of shape coexistence has been found by Azaiez *et al.* [10]. A possible shrinking of the shell-closure feature has also been suggested from the comparison of the measured and calculated solar nuclear abundances for heavy elements. Network calculations for the solar isotopic abundances coming from the rapid neutron-capture processes involved in the explosive stellar nucleosynthesis reproduce the three peaks observed at $A \approx 80$, 130 and 195 if, for very neutron-rich nuclei, the magic neutron numbers are less pronounced than assumed from nuclear structure studies [11].

The $N=50$ shell gap has been predicted to be quenched already at $Z\approx32$ by calculations using mass predictions from the infinite nuclear matter model [5]. Experimental evidence for setting up of collectivity was shown by Kratz *et al.* [12] in the $N=49$ ^{80}Ga from the decay of the r-process waiting-point isotope $^{80}_{30}$Zn$_{50}$. Here the gross β-decay properties as

well as the quasiparticle structure have been interpreted as a clear indication of shape coexistence in ^{80}Ga suggesting a rather rapid weakening of the shell strength far from β stability around ^{78}Ni. This conclusion somewhat contradicts the observation by Daugas *et al.* [13] of an 8^+ isomeric state in ^{78}Zn($N=48$) with a deduced $B(E2, 8^+ \rightarrow 6^+)$ value well reproduced by large scale shell-model calculations.

Predictions of various theoretical models for the $N=50$ isotones also come to differing conclusions. Hartree–Fock–Bogoliubov (HFB) calculations based on Gogny's two-body effective interaction [14] and shell-model calculations [13] predict a persistence of the shell closure for the $N=50$ nuclei close to ^{78}Ni. In contrast a more recent HFB calculation [15], in which pairing (with a density dependent particle-particle interaction) is treated on the same footing as particle-hole interactions, predicts a significant reduction of the shell gap. In such calculations the two neutron separation energy at $N=50$ drops from 18 MeV for Sr ($Z=38$) (on the line of stability) to 11 MeV for Ge ($Z=32$) and then below 8 MeV for Ni ($Z=28$).

In this paper we report on a study of the excited structures of some $N=50$ neutron-rich nuclei. New experimental information has been obtained on the Rb, Br, Se and Ge isotones. The low- and medium-spin structures have been populated using deep-inelastic reactions. The excited states observed in their decay have been compared with shell-model calculations allowing neutron particle-hole excitations across the neutron core. The comparison between measured and calculated excitation energies of the levels at different spin values is used here to investigate the microscopic configuration of such nuclear systems as well as to test the $N=50$ shell gap and its stability down to $Z=32$. Preliminary results from this work, not overlapping with the ones presented here, have been reported in conference proceedings [16].

II. EXPERIMENTAL DETAILS

Excited states of the $^{87}_{37}$Rb, $^{85}_{35}$Br, $^{84}_{34}$Se and $^{82}_{32}$Ge nuclei have been populated using heavy-ion multi-nucleon transfer reactions and studied through γ-ray spectroscopy in a "thick target" measurement [17,18]. The combination of the Tandem-XTU and the superconducting LINAC ALPI accelerators at the Laboratori Nazionali di Legnaro, Italy, was used to accelerate a beam of ^{82}Se ions at an energy of 460 MeV onto a target of ^{192}Os. The target, isotopically enriched to 97.8%, was of a thickness of 60 mg/cm^2, sufficient to stop all reaction fragments. The beam-target combination was chosen in order to maximize the production of the nuclei of interest assuming an N/Z ratio equilibration in deep inelastic processes [18,19]. Our expectation therefore was that the distribution of projectile-like products would be shifted toward more neutron-rich nuclei.

Triple and higher fold γ-γ coincidences were acquired with the 4π spectrometer GASP [20] consisting of 40 Compton-suppressed, large-volume germanium detectors and of an inner BGO ball acting as a multiplicity filter and total-energy spectrometer. Events were collected on tape during six days of beam time under the conditions that a minimum of three Compton-suppressed Ge detectors and two

BGO elements from the multiplicity filter fired in coincidence. With a beam current of 2 particle nA, the event rate was $\sim$4 kHz and the singles rate in each germanium detector $\sim$2 kHz. With such a setup γ rays from the deexciting, target-like and projectile-like fragments were detected. After gain matching for all the detectors, the coincidence data were sorted into fully symmetrized matrices and cubes for subsequent off-line analysis. Since all recoiling fragments were stopped in the target, Doppler broadening prevented the observation of transitions deexciting short-lived states and only γ decays with lifetimes longer than the slowing-down time of the recoiling nuclei ($\sim$1 ps) could be resolved. Thus, no Doppler correction was applied when sorting the data. Isotopic assignments of new γ rays were based on previously reported double-coincidence events. In cases where only one excited state and therefore only the γ ray depopulating it was known, as for ^{85}Br and ^{82}Ge, γ rays have been assigned based on the cross-coincidence relationship with the binary products and according to the expected systematic behavior. Due to the large number of final nuclei produced in the reaction, the isotopic assignments for the observed γ cascades in such cases have to be taken as tentative.

The spins and parities of the levels were deduced, where possible, from angular distribution ratios from oriented states (ADO) as well as from the decay branches. In order to obtain multipolarity information for the emitted γ rays, two asymmetric coincidence matrices were constructed using the γ rays detected at all angles (y axis) against those observed at 34° (or 146°) and 90° (x axes), respectively. In these two matrices, γ-ray intensities in the projected spectrum on the y axis can be regarded as independent from the angular distribution effects of the emitted γ rays. The anisotropies of the emitted γ rays are reflected in the ADO ratios defined as $R_{\mathrm{ADO}}(\gamma)=I_\gamma(34°)/I_\gamma(90°)$. The γ-ray intensities $I_\gamma(34°)$ and $I_\gamma(90°)$ can be extracted from the coincidence spectra using a gating transition (on the y axis) of any multipolarity. In such an analysis stretched quadrupole/dipole transitions should have the ADO ratios larger/smaller than unity ($\approx$1.4 for pure quadrupole and $\approx$0.8 for pure dipole). It should be noted that uncertainties occur for the spin and parity assignments on the basis of ADO ratio analysis; the stretched quadrupole transitions cannot be distinguished from $\Delta I=0$ dipole transitions or certain E2/M1 admixtures of $\Delta I=1$ transitions. In these cases, cross checks from crossover or parallel transitions and their branching ratios provide supplementary arguments for spin and parity assignments. The measured spectroscopic data (γ-ray energies, relative intensities, ADO ratios where possible, and suggested spin assignments) are summarized in Tables I–IV for the four nuclei discussed in this paper.

III. EXPERIMENTAL RESULTS

From the analysis of single- and double-gated spectra, previously unidentified γ rays have been assigned to the $N=50$ isotones $^{87}_{37}$Rb, $^{85}_{35}$Br, $^{84}_{34}$Se and $^{82}_{33}$Ge. Due to the nature of the binary reaction mechanism used to populate such nuclei, in all cases the cross γ-ray coincidences (the γ rays coming from the decay of the "target-like" fragments in coincidence

TABLE I. The γ-ray transition energies, relative intensities, ADO ratios, and level assignments for the ^{87}Rb nucleus.

E_γ(keV)[a]	I_γ[b]	R_{ADO}	$E_i \rightarrow E_f$(keV)[c]	$J_i^\pi \rightarrow J_f^{\pi}$[d]
171.7	33	0.60(7)	$5027 \rightarrow 4855$	$21/2^{(+)} \rightarrow 19/2^{(+)}$
235.0	54	0.56(6)	$3644 \rightarrow 3409$	$15/2^{(+)} \rightarrow 13/2^+$
255.8	7		$6822 \rightarrow 6566$	
402.6	100	1.05(6)	$403 \rightarrow 0$	$5/2^- \rightarrow 3/2^-$
408.0	7		$3409 \rightarrow 3001$	$13/2^{(+)} \rightarrow 11/2^{(+)}$
454.5	19	0.95(28)	$5481 \rightarrow 5027$	$23/2^{(+)} \rightarrow 21/2^{(+)}$
506.6	50	0.79(10)	$4151 \rightarrow 3644$	$17/2^{(+)} \rightarrow 15/2^{(+)}$
704.4	26	1.29(20)	$4855 \rightarrow 4151$	$19/2^{(+)} \rightarrow 17/2^{(+)}$
875.9	7		$5027 \rightarrow 4151$	$21/2^{(+)} \rightarrow 17/2^{(+)}$
1084.7	7		$6566 \rightarrow 5481$	$\rightarrow 23/2^{(+)}$
1175.3	74	1.02(7)	$1578 \rightarrow 403$	$9/2^+ \rightarrow 5/2^-$
1211.0	7		$4855 \rightarrow 3644$	$19/2^{(+)} \rightarrow 15/2^{(+)}$
1340.5	7		$6822 \rightarrow 5481$	$\rightarrow 23/2^{(+)}$
1423.0	7		$3001 \rightarrow 1578$	$(11/2^+) \rightarrow 9/2^+$
1831.1	63	1.13(7)	$3409 \rightarrow 1578$	$13/2^+ \rightarrow 9/2^+$

[a]Uncertainties are between 0.1 and 0.5 keV.
[b]Intensities are normalized to the 402.6 keV line. Uncertainties are within 20%.
[c]Excitation energies of initial E_i and final E_f states.
[d]Proposed spin and parity assignments for the initial I_i^π and final I_f^π levels.

with those coming from the "beam-like" reaction products) were used to distinguish between the different reaction partners. Examples of coincidence spectra for the nuclei of interest are presented in Figs. 1–3.

A. ^{87}Rb

The few previously reported excited states in $^{87}_{37}$Rb come from a variety of experiments including particle transfer re-

TABLE II. The γ-ray transition energies, relative intensities, ADO ratios, and level assignments for the ^{85}Br nucleus.

E_γ(keV)[a]	I_γ[b]	R_{ADO}	$E_i \rightarrow E_f$(keV)[c]	$J_i^\pi \rightarrow J_f^{\pi}$[d]
296.9	6		$2733 \rightarrow 2437$	$13/2^+ \rightarrow (11/2^+)$
345.2	100	1.10(9)	$345 \rightarrow 0$	$5/2^- \rightarrow 3/2^-$
382.6	30	0.80(23)	$3709 \rightarrow 3327$	$17/2^{(+)} \rightarrow 15/2^{(+)}$
593.5	63	0.90(16)	$3327 \rightarrow 2733$	$15/2^{(+)} \rightarrow 13/2^+$
633.7	26		$4343 \rightarrow 3709$	$(19/2^+) \rightarrow 17/2^{(+)}$
864.5	14		$2437 \rightarrow 1573$	$(11/2^+) \rightarrow 9/2^+$
1160.7	43	1.25(36)	$2733 \rightarrow 1573$	$13/2^+ \rightarrow 9/2^+$
1227.3	92	1.30(10)	$1573 \rightarrow 345$	$9/2^+ \rightarrow 5/2^-$

[a]Uncertainties are between 0.1 and 0.5 keV.
[b]Intensities are normalized to the 345.2 keV line. Uncertainties are within 20%.
[c]Excitation energies of initial E_i and final E_f states.
[d]Proposed spin and parity assignments for the initial I_i^π and final I_f^π levels.

TABLE III. The γ-ray transition energies, relative intensities, ADO ratios, and level assignments for the ^{84}Se nucleus.

E_γ(keV)[a]	I_γ[b]	R_{ADO}	$E_i \rightarrow E_f$(keV)[c]	$J_i^\pi \rightarrow J_f^{\pi}$[d]
164.7	7	0.60(10)	$3702 \rightarrow 3537$	$6^+ \rightarrow (5^+)$
492.0			$3863 \rightarrow 3371$	$\rightarrow (5^-)$
667.0	92	1.37(5)	$2122 \rightarrow 1455$	$4^+ \rightarrow 2^+$
704.3	12		$4406 \rightarrow 3702$	$(7^+) \rightarrow 6^+$
1249.0	11		$3371 \rightarrow 2122$	$\rightarrow 4^+$
1415.3	28	1.40(15)	$3537 \rightarrow 2122$	$(5^+) \rightarrow 4^+$
1454.7	100	1.34(7)	$1455 \rightarrow 0$	$2^+ \rightarrow 0^+$
1580.2	18	1.56(22)	$3702 \rightarrow 2122$	$6^+ \rightarrow 4^+$

[a]Uncertainties are between 0.1 and 0.5 keV.
[b]Intensities are normalized to the 1454.7 keV line. Uncertainties are within 20%.
[c]Excitation energies of initial E_i and final E_f states.
[d]Proposed spin and parity assignments for the initial I_i^π and final I_f^π levels.

actions [21–24], β-decay experiments [25,26], (n,n') reaction [27], Coulomb excitation [28], inelastic proton [29] and α-particle scattering [30] and a very recent (γ,γ') reaction study [31]. The $I^\pi=9/2^+$ state at 1578 keV excitation energy was the level with the highest angular momentum known prior to our experiment. It is interpreted as the proton $g_{9/2}$ single-particle state (see Fig. 4). In the present work, by using the coincidence relationship between the two γ-ray transitions of 1175.3 and 402.6 keV deexciting the $9/2^+$ state to the ground state, we have extended the level scheme of ^{87}Rb to an excitation energy of $E=6.8$ MeV as shown in Fig. 4. The assignments of $I^\pi=5/2^-$ and $9/2^+$ to the levels at 403 and 1578 keV excitation energy come from previous studies [32] and are confirmed in our work. The level at 3409 keV deexcites through a 1831.1 keV transition, observed in the double-gated spectrum in coincidence with the 1175.3 and 402.6 keV γ rays. An $I^\pi=13/2^+$ assignment is suggested in

TABLE IV. The γ-ray transition energies, relative intensities, ADO ratios, and level assignments for the ^{82}Ge nucleus.

E_γ(keV)[a]	I_γ[b]	R_{ADO}	$E_i \rightarrow E_f$(keV)[c]	$J_i^\pi \rightarrow J_f^{\pi}$[d]
(681.0)[e]	10		$2028 \rightarrow 1348$	$(4^+) \rightarrow (2^+)$
866.2	12		$2214 \rightarrow 1348$	$(2^+) \rightarrow (2^+)$
1347.6	100		$1348 \rightarrow 0$	$(2^+) \rightarrow 0^+$
(1577.5)[e]	18		$3606 \rightarrow 2028$	$(6^+) \rightarrow (4^+)$
(1468.0)			$3682 \rightarrow 2214$	$\rightarrow (2^+)$

[a]Uncertainties are between 0.1 and 0.5 keV.
[b]Intensities are normalized to the 1347.6 keV line. Uncertainties are within 30%.
[c]Excitation energies of initial E_i and final E_f states.
[d]Proposed spin and parity assignments for the initial I_i^π and final I_f^π levels.
[e]Transition observed in double coincidence with the 1347.6 keV line of ^{82}Ge and with the 316.5 keV γ ray of the binary reaction partner $(-2p+2n)^{192}$Pt but also present in ^{87}Kr (not in coincidence with the 1347.6 keV γ transition).
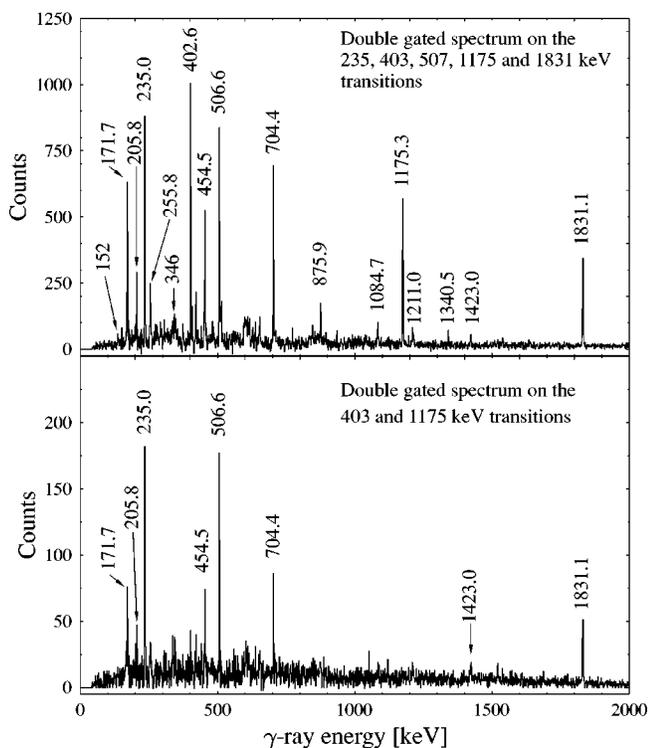
FIG. 1. Coincidence spectra for ^{87}Rb. Top: Summed spectrum double gated on the 235.0, 402.6, 506.6, 1175.3 and 1831.1 keV transitions. Bottom: Double-gated spectrum on the previously known 402.6 and 1175.3 keV transitions. Two γ-ray lines of 152 and 346 keV are observed in double-gated coincidence with the major transitions in ^{87}Rb; they are tentatively assigned to the binary partner ^{187}Ta. The 205.8 keV line is from the target nucleus ^{192}Os (random coincidence).

FIG. 2. Coincidence spectra for ^{85}Br. Top: Summed spectrum double-gated on the 345.2, 593.5, 1160.7 and 1227.3 keV lines (the 205.8 keV line is from ^{192}Os-random coincidence). Bottom: Double-gated spectrum on the 1227.3 keV transition assigned to ^{85}Br and on the 258.0 keV transition belonging to the binary partner ^{189}Re. The 345.2 keV line as well as the other γ-ray lines proposed for ^{85}Br are clearly visible.

the current work for this level based on the value of the ADO ratio of the 1831.1 keV transition, reported in Table I. This value, as well as the one obtained for the 1175.3 keV line, is somewhat smaller with respect to the expected value for an $E2$ stretched transition (≈ 1.4). This is probably related to a reduction in alignment due to higher lying isomeric states. A decay branch parallel to the 1831.1 keV transition is observed in the double-gated spectrum in coincidence with the 402.6 and 1175.3 keV γ rays. This identifies a level at 3001 keV which, on the basis of systematics, is assigned as $I^{\pi}=(11/2^{+})$. A 235.0 keV γ-ray transition deexcites a level at 3644 keV to the $13/2^{+}$ state. The corresponding ADO value clearly indicates a mixing, with a negative δ, suggesting an $M1$ multipolarity for the 235.0 keV transition and therefore a $15/2^{(+)}$ assignment for the 3644 keV level. The ADO values obtained for the 704.4, 171.7, and 454.5 keV γ rays are all compatible with the values expected for $M1/E2$ transitions with relatively strong mixing. The 506.6 keV line appears as a pure dipole transition. Assignments of $17/2^{(+)}$, $19/2^{(+)}$, $21/2^{(+)}$ and $23/2^{(+)}$ are proposed for the states at 4151, 4855, 5027 and 5481 keV, respectively. The observed crossover transitions of 876.0 and 1211.0 keV deexciting the 5027 and the 4855 keV levels support such assignments. The two levels observed at 6566 and 6822 keV excitation energies are too weakly populated to allow us to extract the ADO values for the two transitions which deexcite them to the 5481 keV
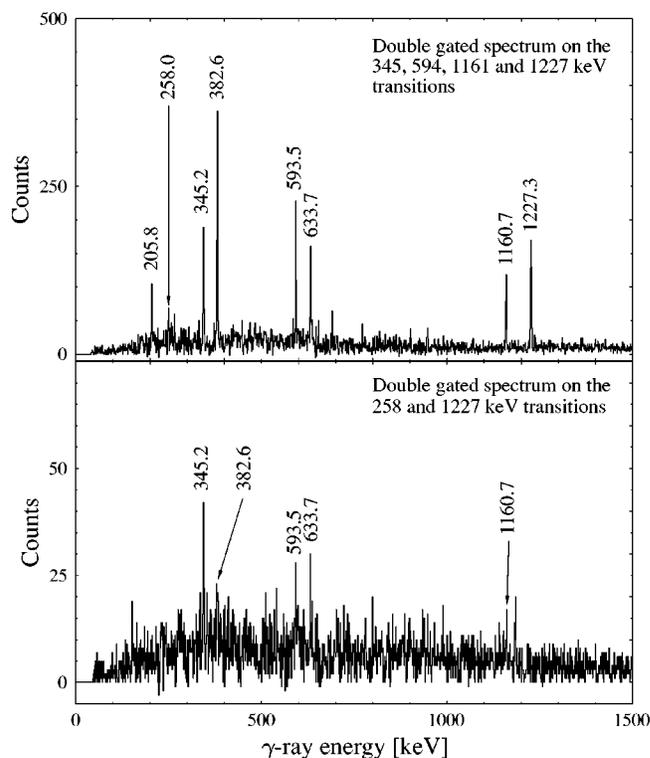
state. Accordingly, no spin and parity assignments can be proposed in the current work.

B. ^{85}Br

In the $N=50$, $^{85}_{35}$Br nucleus only states with spins up to $I=7/2$ were known in the literature, coming from β-decay
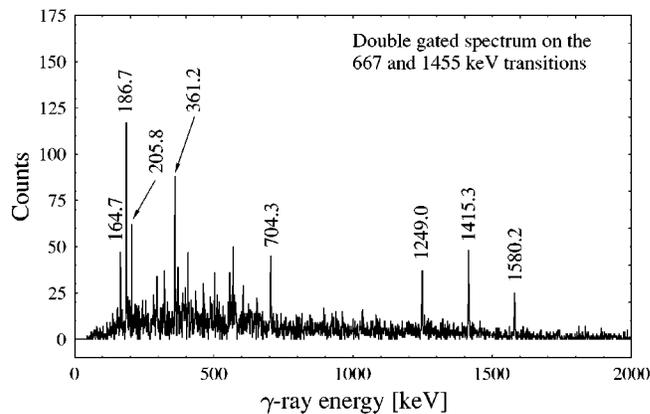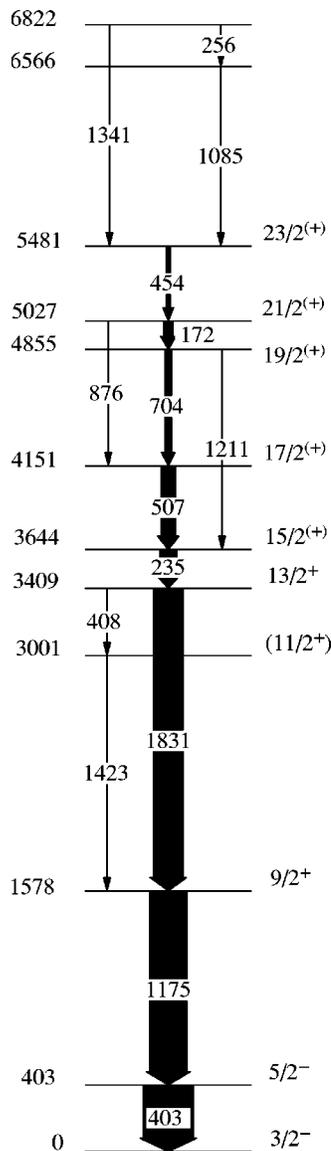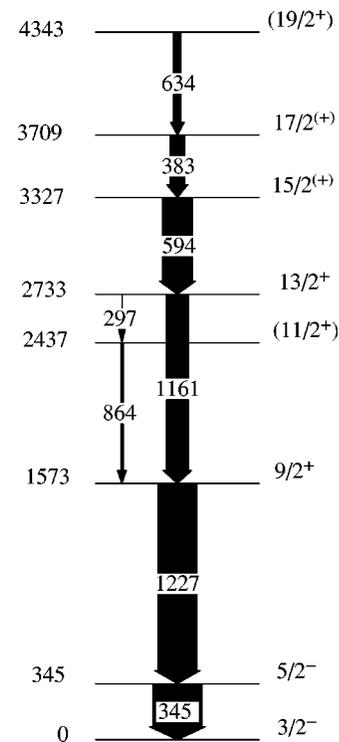

FIG. 3. Coincidence spectrum for ^{84}Se, double gated on the 667.0 and 1454.7 keV lines. The 205.8 keV line is from the target nucleus ^{192}Os, the 186.7 and 361.2 γ-ray transitions are from the binary partner ^{190}Os (random coincidence).

FIG. 4. Level scheme of ^{87}Rb deduced from this work.

FIG. 5. Level scheme of ^{85}Br deduced from this work.

and direct-reaction studies [32]. Since the excitation energy of the $9/2^+$ yrast state, expected below 2 MeV, was unknown, the isotopic identification of the γ cascades deexciting levels in ^{85}Br could only be based on a single-gating condition on the 345.2 keV $5/2^- \rightarrow 3/2^-$ γ transition. After a detailed analysis of all γ rays in coincidence, candidate transitions were checked by setting double gastes on the 345.2 keV $5/2^- \rightarrow 3/2^-$ line of $^{85}_{35}$Br and on the 258 keV, $3/2^+ \rightarrow 5/2^-$ transition in the binary partner ^{189}Re [32]. An essential ingredient in the isotopic determination was the use of triple γ coincidences which allowed us to select each "projectile-like"-target-like combination. Once a few γ rays were identified the level scheme was built up by setting multiple-gate conditions. The final level scheme, reported in Fig. 5, has been extended up to an excitation energy of 4.343 MeV. Seven γ rays have been placed above the 345 keV $5/2^-$ level and ordered on the basis of the observed intensity relations. The state at an excitation energy of 1573 keV, close to the expected value of the $9/2^+$ excitation,

decays to the 345 keV, $5/2^-$ level via a 1227.3 keV γ-ray line. The ADO result for this γ-ray transition is compatible with a $\Delta I=2$ multipolarity (see Table II) thus supporting a $9/2^+$ assignment for the 1573 keV state. This level is fed by a 1160.7 keV line deexciting the 2733 keV level. The ADO result here is also compatible with a $\Delta I=2$ multipolarity supporting a $13/2^+$ assignment for this level. A decay branch parallel to the 1160.7 keV γ-ray line is observed in the double-gated spectrum in coincidence with the 345.2 and 1227.3 keV γ rays. This identifies a new level at 2437 keV excitation energy for which, as in the similar case of ^{87}Rb, an $I^\pi=(11/2^+)$ assignment is preferred.

The ADO ratios for the 593.5 and 382.6 keV transitions are consistent with pure $\Delta I=1$ multipolarities. We prefer $15/2^{(+)}$ and $17/2^{(+)}$ spin and parity assignments for the levels at 3327 and 3709 keV in analogy to the corresponding levels in ^{87}Rb. The level identified at 4343 keV in excitation energy which decays to the 3709 keV level via a 633.7 keV transition is too weakly populated to extract an ADO value. The $(19/2^+)$ assignment for this state, reported in Table II, is based on systematics (see corresponding level in ^{87}Rb).
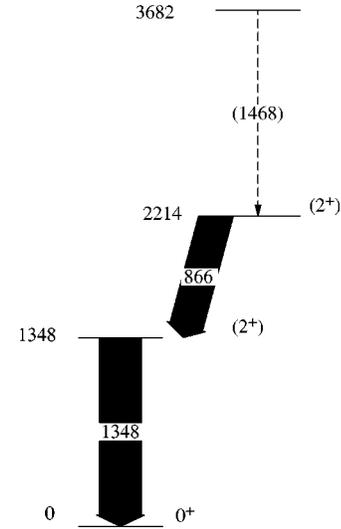
C. ^{84}Se

The $N=50$ nuclide $^{84}_{34}$Se has been studied prior to the present work in β-decay [33] and (t,p) [34,35] reactions. The highest spin state reported to date is $I=4$. Accordingly we have used the spectra double gated on the 1454.7 keV, $2^+ \rightarrow 0^+$ and 667.0 keV, $4^+ \rightarrow 2^+$ transitions for the identification of the other γ rays. The level scheme has been extended up to $I=(7^+)$ at an excitation energy of 4.4 MeV as shown in Fig. 6. The values obtained from the ADO analysis have
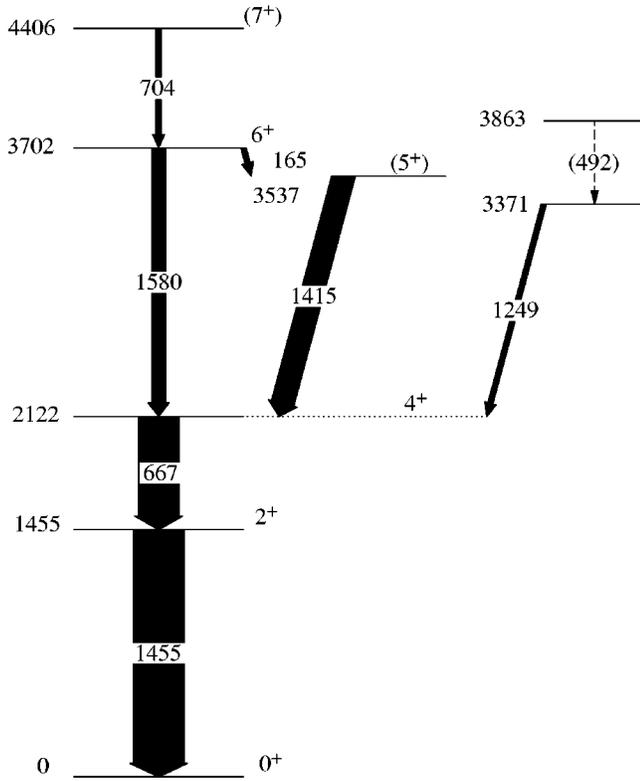
FIG. 6. Level scheme of ^{84}Se deduced from this work.

FIG. 7. Level scheme of ^{82}Ge deduced from this work.

confirmed the assignments known from previous works for the $I^{\pi}=2^+$ and 4^+ states at 1455 and 2122 keV, respectively. The 6^+ state at 3702 keV has been assigned on the basis of both the decay pattern and the ADO value extracted for the 1580.2 keV transition. For the level at 3537 keV in excitation energy a (5^+) assignment is preferred based on the ADO value of the 164.7 keV γ ray (typical of a $\Delta I=1$ transition with a large mixing and therefore of magnetic character) and on the ADO result for the 1415.3 keV γ ray (which is compatible with an $M1/E2$ mixed multipolarity). The low intensity of the 1249.0, 492, and 704.3 keV transitions did not allow us to extract ADO values. Therefore the spin and parity assignment for the 4406 keV level suggested here is based on systematics having as a reference the $N=50$ ^{86}Kr nucleus [32].

D. ^{82}Ge

The only information available concerning $^{82}_{32}$Ge comes from β-decay studies [36] and is limited to two levels with $I^{\pi}=(2^+)$. These spin assignments are based on β-decay rates and on the observation of a 2214 keV line deexciting the (2^+_2) level to the ground state. Both levels are also observed in our experiment but the low intensity of the 866.2 and 1347.6 keV transitions deexciting the (2^+_2) to the (2^+_1) and the latter to the ground state did not allow us to extract the ADO values. Gating on both γ lines a possible level at 3682 keV was observed. In order to identify the higher-spin states of ^{82}Ge we have analyzed any γ-ray transition observed in coincidence with the 1347.6 keV$(2^+)\rightarrow 0^+$ transition. Any candidate γ-ray transition was checked using double-gating con-

ditions for detecting coincident γ rays. All the γ cascades selected in this way were checked to ensure that they do not belong to other nuclei. In order to verify our identification we also used a cross-coincidence analysis with γ rays from the target-like partner. Two coincident γ rays of 681.0 and 1577.5 keV fulfilled all the required conditions, being in coincidence with both the 1347.6 keV transition from ^{82}Ge and the 316.5 keV, $2^+\rightarrow 0^+$ transition in the binary product ($-2p+2n$) ^{192}Pt [32]. Two γ rays with these energies are known to be in mutual coincidence in the decay scheme of ^{87}Kr, but they do not decay through a 1348 keV γ-ray transition. Accordingly we tentatively propose the assignment of such a γ lines to ^{82}Ge (see Table IV) but, due to the uncertainty related to the contaminant γ lines, we prefer not to include them in the proposed level scheme shown in Fig. 7. Due to the low cross section for this reaction channel ($-2p+2n$), which is estimated to be of the order of $\approx 10\ \mu$b, we could not extract any multipolarity information. Therefore, the spins and parities of the levels are assigned on the basis of systematics [32] (Fig. 7).

IV. SHELL-MODEL CALCULATIONS

Shell-model calculations have been performed using the RITSSCHIL [37] code. Two sets of calculations have been carried out, one allowing (SM2) particle-hole excitations across the $N=50$ neutron core and the other (SM1) not. The shell-model space used includes the active proton orbitals $\pi(0f_{5/2},1p_{3/2},1p_{1/2},0g_{9/2})$ and neutron orbitals $\nu(1p_{1/2},0g_{9/2},1d_{5/2})$ relative to a hypothetical $^{66}_{28}$Ni$_{38}$ core. Since an empirical set of effective interaction matrix elements for this model space is not available yet, various empirical sets have been combined with values obtained using a modified surface-delta interaction. Details of this last procedure are described in Refs. [38,39]. The effective interaction in the proton shells was taken from Ref. [40], where the residual interaction and the single-particle energies of the proton orbitals were deduced from a least-squares fit to 170

experimental level energies in the $N=50$ nuclei with mass numbers between 82 and 96. For the proton-neutron interaction between the $\pi(1p_{1/2}, 0g_{9/2})$ and the $\nu(1p_{1/2}, 0g_{9/2})$ orbitals the data of Ref. [41] have been used. They were derived from an iterative fit to 95 experimental level energies of the $N=48$, 49 and 50 nuclei. The matrix elements of the neutron-neutron interaction of the $\nu(1p_{1/2}, 0g_{9/2})$ orbitals have been assumed to be equal to the isospin $T=1$ component of the proton-neutron interaction given in Ref. [41]. For the $(\pi 0f_{5/2}, \nu 0g_{9/2})$ residual interaction, the matrix elements proposed in Ref. [24] have been used.

The single-particle energies relative to the ^{66}Ni core were derived from the single-particle energies of the proton orbitals given in Ref. [40] with respect to the doubly magic $^{78}_{28}$Ni$_{50}$ core and from the neutron single-hole energies of the $1p_{1/2}, 0g_{9/2}$ orbitals [41]. The transformation of these single-particle energies to those relative to the ^{66}Ni core was performed [42] on the basis of the effective residual interactions given above. The obtained values, in MeV, are $\epsilon^{\pi}_{0f_{5/2}}=-9.106$, $\epsilon^{\pi}_{1p_{3/2}}=-9.033$, $\epsilon^{\pi}_{1p_{1/2}}=-4.715$, $\epsilon^{\pi}_{0g_{9/2}}=-0.346$, $\epsilon^{\nu}_{1p_{1/2}}=-7.834$, $\epsilon^{\nu}_{0g_{9/2}}=-6.749$, $\epsilon^{\nu}_{1d_{5/2}}=-4.144$.

To make the calculation feasible, a truncation of the occupation numbers was necessary. At most, three protons were allowed to occupy the $1p_{1/2}, 0g_{9/2}$ orbitals and no more than one $0g_{9/2}$ neutron was allowed to be excited to the $1d_{5/2}$ orbital (SM2). In order to test the role of the $g_{7/2}$ orbit in the calculation, in some cases, where the limited particle number has allowed it, we have added it to the neutron configuration space. The results obtained were practically uneffected by the inclusion of such orbit as a consequence of the very small occupation factor.

V. DISCUSSION

We report here on four $N=50$ isotones, namely $^{87}_{37}$Rb, $^{85}_{35}$Br, $^{84}_{34}$Se and $^{82}_{32}$Ge. The study of how their excited structures evolve as a function of the proton number, performed through the comparison with shell-model predictions obtained assuming a closed $N=50$ core, can be taken as a test of the persistence (or not) of the neutron shell gap when moving away from the line of β stability. Such a comparison shows the importance of the breakup of the neutron core through particle-hole excitations across a constant $N=50$ gap, for the description of medium- and high-spin excitations ($I \approx 8$). It is worth mentioning here that a similar shell-model analysis performed for the $N=48$ Se and Ge isotones (which will be reported in a forthcoming publication [43]) results in a reasonable reproduction of the excited energy levels in the above-mentioned spin region without requiring a breaking of the closed neutron-core (and is therefore insensitive to a possible modification of the neutron shell gap). The fact that the shell-model description seems to reproduce the observed spectra can be considered as evidence for an adequate description of the residual nucleon-nucleon interaction and of the single-particle energies (shell gap), thus indicating a continued stability of the $N=50$ shell gap in the vicinity of $^{78}_{28}$Ni.

A. Nucleus ^{87}Rb

A comparison of the experimental and calculated levels of $^{87}_{37}$Rb is shown in Fig. 8. Two calculations have been carried
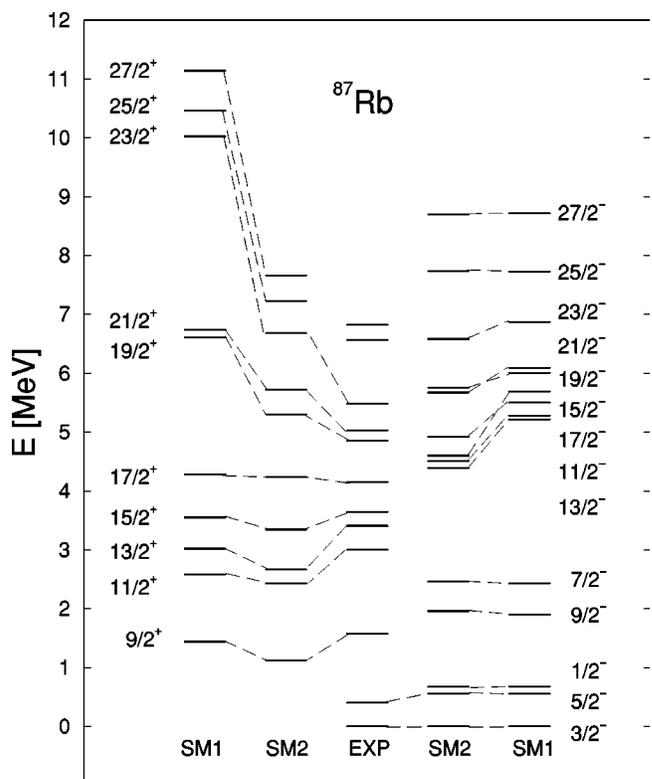

FIG. 8. Shell model calculation for ^{87}Rb. The calculations are performed using either a proton space (SM1) or allowing also particle-hole excitations across the $N=50$ shell gap (SM2). The experimental results from the present study are also reported for comparison.

out. The first (SM1) has been performed using only a proton configuration space, the second (SM2) allowing excitations across the $N=50$ neutron shell gap from the $0g_{9/2}$ into the $1d_{5/2}$ orbits. The excitation energies of all experimentally known levels up to spin $I^{\pi}=17/2^{+}$ are well reproduced using only the proton configuration space (SM1). The $3/2^{-}$ ground state and the $5/2^{-}$ first excited level show a structure consisting mainly of a single proton particle in the $1p_{3/2}$ or a proton hole in the $0f_{5/2}$, orbit, respectively. The next excitation requires a promotion of a proton particle into the $0g_{9/2}$ state. Such a state will couple with the proton-core excitations giving rise to the positive-parity excitations up to the $17/2^{+}$ state at 4.1 MeV of excitation energy. All those energy values compare reasonably with the shell-model predictions calculated using only the proton-configuration space. Above 4.1 MeV the agreement between the experimental levels and the shell-model calculations performed in the proton space (SM1) becomes rather poorer. It is likely that at this point particle-hole excitations across the $N=50$ neutron core begin to be important. In fact, by comparing the measured values with the excited levels calculated using both the proton and neutron spaces (SM2) the agreement between experimental and calculated energies above 4.1 MeV improves significantly (see SM2 in Fig. 8). A closer inspection of the wave functions involved shows that the dominant contributions to the $19/2^{+}$, $21/2^{+}$ and $23/2^{+}$ states at excitation energies of 4855, 5027 and 5481 keV, respectively, result from coupling
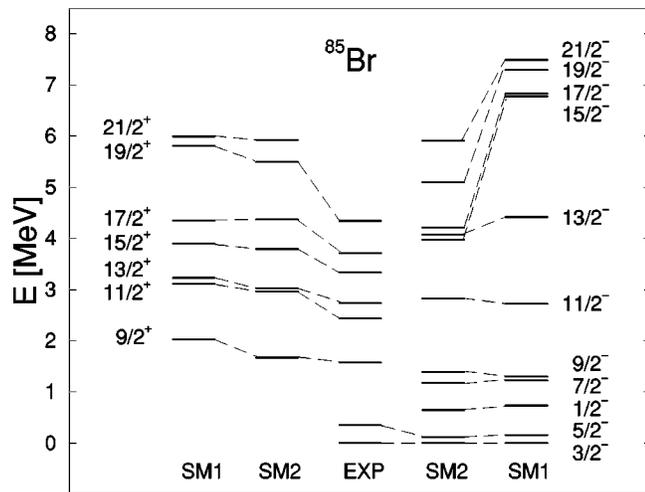
FIG. 9. Shell model calculation for ^{85}Br. The calculations are performed using either a proton space (SM1) or allowing also particle-hole excitations across the $N=50$ shell gap (SM2). The experimental results from the present study are also reported for comparison.

FIG. 10. Shell model calculation for ^{84}Se. The calculations are performed using either a proton space (SM1) or allowing also particle-hole excitations across the $N=50$ shell gap (SM2). The experimental results from the present study are also reported for comparison.

the neutron cluster $\nu(0g_{9/2}^{-1}, 1d_{5/2}^1)_j$ to the proton particle excitations. A similar structure has been suggested at high spin in Ref. [38] for the $N=50$ $^{86}_{36}$Kr nucleus. We note, however, that, even if the general agreement between observed and calculated (SM2) level energies in this excitation energy region is remarkable, the value obtained for the calculated excitation energies of the yrast levels are somewhat too high. Such disagreement perhaps indicates that part of the collectivity is still missing from the description. For the higher-lying states at 6566 and 6822 keV, definitive spin and parity assignments were not possible in the present experiment. Thus, these states might be compared with calculated levels of either positive or negative parity.

B. Nucleus ^{85}Br

The comparison of the experimental and calculated levels for $^{85}_{35}$Br basically shows results similar to $^{87}_{37}$Rb. Figure 9 shows the experimental and calculated (using both the proton-SM1– and the proton-neutron–SM2– configuration spaces) energy spectra for ^{85}Br. Here also the $3/2^-$ ground state and the $5/2^-$ first excited state show a structure based on a proton hole in the $1p_{3/2}$ or the $0f_{5/2}$ orbit, respectively. Interestingly the $0g_{9/2}$ proton excitation is found at an excitation energy of 1573 keV, only 5 keV lower than that of the similar state in $^{87}_{37}$Rb. The excitation energies of the shell-model states above the $9/2^+$ level calculated in the proton configuration space (SM1) are much too high compared to the experimental ones. A better agreement is obtained when neutron excitations across the $N=50$ shell gap are allowed (SM2), even if the calculated energy spectrum is still too high with respect to the measured one. This indicates that core breaking particle-hole components become important above the $9/2^+$ as shown by the lowering in excitation energy of the $11/2^+$ or $19/2^+$ states in SM2 with respect to SM1 as well as of the negative parity levels. Nevertheless,
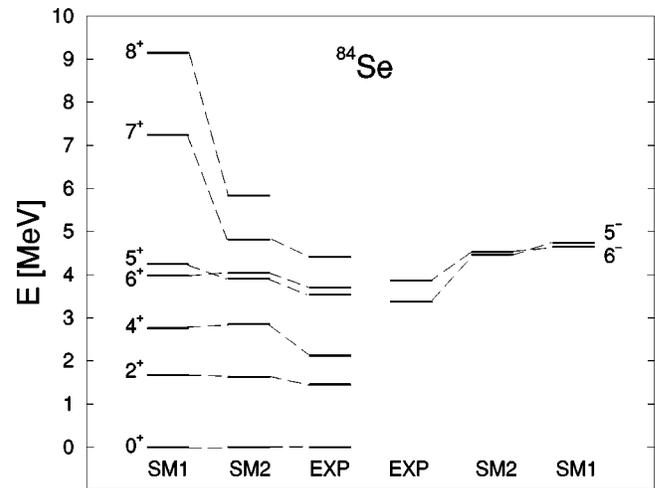
the effect of such core-breaking excitations on the excitation energies of the states seems here somewhat more limited when compared to $^{87}_{37}$Rb.

C. Nucleus ^{84}Se

In the $^{84}_{34}$Se nucleus most of the observed levels are reasonably reproduced within the proton configuration space (SM1 in Fig. 10) up to spin $I^\pi=6^+$ at 3.7 MeV excitation energy. The only exception is the 4^+ state which is calculated to be too high in our parametrization; for this state the configuration $(0f_{5/2}^{-1}, 1p_{3/2}^1)$ is predicted to be the main component. The 6^+ state at 3702 keV is also reasonably reproduced within the proton space (SM1); the correct ordering of the 5^+ and 6^+ levels is only reproduced in the (SM2) space indicating the presence of significant components containing the $\nu(0g_{9/2}^{-1}, 1d_{5/2}^1)$ configuration (see Fig. 10). As in the previous Rb and Br cases, the presence of neutron-core excitations above 3.7 MeV excitation energy is more clearly indicated by the drastic lowering in excitation energy, with respect to the value calculated using only the proton space (SM1), of the calculated $I^\pi=7^+$ and 8^+ states in the neutron space (SM2). The comparison between experimental and calculated (SM2) levels shows a good general agreement even though the 7^+ state is predicted at somewhat too high an energy, indicating that part of the collectivity is missing due to the restriction of the shell model basis.

D. Nucleus ^{82}Ge

Figure 11 shows the comparison of experimental and calculated levels in $^{82}_{32}$Ge. Due to the very limited experimental information only the low spin region can be discussed here. Good agreement is observed between the experimental level energies and those calculated using only the proton space (SM1). The calculated excitation energies of the 2^+ and 4^+ states are basically unaffected by the inclusion of the
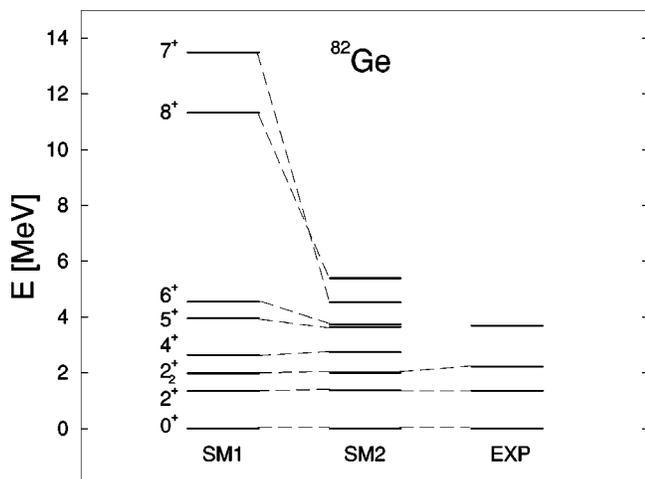
FIG. 11. Shell model calculation for ^{82}Ge. The calculations are performed using either a proton space (SM1) or allowing also particle-hole excitations across the *N*=50 shell gap (SM2). The experimental results from the present study are also reported for comparison.

stricted particle space. In particular, the pairing excitations across the *N*=50 shell are only partially accounted for by the monopole part of the shell model interaction. The increase in such deviations when reducing the proton number supports such an interpretation.

F. Summary

This paper presents the results of an in-beam study of medium- and high-spin states in the *N*=50, $^{87}_{37}$Rb, $^{85}_{35}$Br, $^{84}_{34}$Se and $^{82}_{32}$Ge nuclei populated through the reaction ^{82}Se + ^{192}Os at 460 MeV beam energy. In all these nuclei we could extend the level scheme up to higher spin and excitation energy. The comparison with shell-model calculations has enabled us to test the contribution in the nuclear wave functions of the neutron excitations across the *N*=50 core. The calculations have shown that at least one-particle-one-hole excitations have to be included in the configuration space to get a reasonable description of the excited, positive-parity levels above spin $I=17/2\hbar$ in $^{87}_{37}$Rb and $^{85}_{35}$Br and spin $I=4\hbar$ in $^{84}_{34}$Se and $^{82}_{32}$Ge. Due to the neutron particle-hole contribution to the configurations, the excitation energies of the higher-lying structures are sensitive to the value of the neutron shell gap. The generally good agreement obtained between calculated and measured level energies in all the cases considered is taken as an argument for the proper description of such semimagic nuclei within the shell-model framework and therefore of the persistence of the *N*=50 closed shell down to *Z*=32. The expected shell weakening, possibly manifested through energetically favored intruder configurations and therefore through low-lying configuration or shape coexistence, will probably appear only for higher spin states or for larger values of the *N/Z* ratio.

neutron-core excitations, while the lowering of the calculated 6^+ state in SM2 with respect to the value of SM1 indicates a significant component of the $\nu(0g_{9/2}^{-1}, 1d_{5/2}^1)$ configuration. Note that the proposed (4^+) and (6^+) states at 2028 and 3606 keV of excitation energy respectively (see Table IV) compare well with those calculated following the trend observed in the other *N*=50 isotones.

E. Shell stability at *N*=50

For all *N*=50 nuclei discussed above we have shown that in order to reasonably reproduce the excited levels above $I^\pi=17/2^+$ and 6^+ (for odd-even and even-even systems, respectively), it is necessary to introduce particle-hole excitations across the *N*=50 gap. The size of the gap (about 4 MeV for ^{78}Ni) has been kept constant in the calculations. The general agreement observed between the measured and calculated excitation energies of the levels (see Figs. 8–11) can therefore be considered to be a strong indication that, when moving away from the stability line down to *Z*=32, the *N*=50 gap remains constant. The deviations observed between the calculated and the experimental values at high spin can be attributed to the limited collectivity available in our re-

[1] T. Motobayashi *et al.*, Phys. Lett. B **346**, 9 (1995).
[2] N. A. Orr *et al.*, Phys. Lett. B **258**, 29 (1991).
[3] O. Sorlin *et al.*, Phys. Rev. C **47**, 2941 (1993).
[4] J. Dobaczewski *et al.*, Phys. Scr. **T56**, 15 (1995).
[5] R. C. Nayak, Phys. Rev. C **60**, 064305 (1999).
[6] X. Campi *et al.*, Nucl. Phys. **A251**, 193 (1975).
[7] N. Fukunishi *et al.*, Phys. Lett. B **296**, 279 (1992).
[8] T. Glasmacher *et al.*, Phys. Lett. B **395**, 163 (1997).
[9] H. Scheit *et al.*, Phys. Rev. Lett. **77**, 3967 (1996).
[10] F. Azaiez *et al.*, Nucl. Phys. **A704**, 37c (2002).
[11] B. Chen *et al.*, Phys. Lett. B **355**, 37 (1995).
[12] K. L. Kratz *et al.*, Phys. Rev. C **38**, 278 (1988).
[13] J. M. Daugas *et al.*, Phys. Lett. B **476**, 213 (2000).
[14] M. Girod *et al.*, Phys. Rev. C **37**, 2600 (1988).
[15] T. R. Werner *et al.*, Z. Phys. A **358**, 169 (1997).
[16] Zs. Podolyàk *et al.*, Int. J. Mod. Phys. E **13**, 123 (2004).
[17] R. Broda *et al.*, Phys. Rev. Lett. **68**, 1671 (1992).
[18] W. Krolas *et al.*, Nucl. Phys. **A724**, 289 (2003).

[19] B. Fornal *et al.*, Phys. Rev. C **49**, 2413 (1994).

[20] D. Bazzacco, *Proceedings of the International Conference on Nuclear Structure at High Angular Momentum*, Ottawa, 1992 Vol. II, p. 376, Report No. AECL10613.

[21] J. F. Harrison and J. C. Hiebert, Nucl. Phys. **A185**, 385 (1972).

[22] J. R. Comfort *et al.*, Phys. Rev. C **8**, 1354 (1973).

[23] L. R. Medsker *et al.*, Phys. Rev. C **12**, 1516 (1975).

[24] P. C. Li *et al.*, Nucl. Phys. **A469**, 393 (1987).

[25] A. Shibab-Eldin *et al.*, Nucl. Phys. **A160**, 33 (1971).

[26] F. K. Wohn *et al.*, Phys. Rev. C **7**, 160 (1973).

[27] E. Barnard *et al.*, Z. Phys. A **296**, 295 (1980).

[28] P. D. Bond and G. J. Kumbartzki, Nucl. Phys. **A205**, 239 (1973).

[29] L. Hulstmann *et al.*, Nucl. Phys. **A251**, 269 (1975).

[30] L. Käubler *et al.*, Z. Phys. A **352**, 127 (1995).

[31] L. Käubler *et al.*, Phys. Rev. C **65**, 054315 (2002).

[32] R. B. Firestone, *Table of Isotopes*, 8th ed. (Wiley, New York, 1996).

[33] P. Hoff *et al.*, Z. Phys. A **338**, 285 (1991).

[34] J. D. Knight *et al.*, Phys. Rev. C **9**, 1467 (1974).

[35] S. M. Mullins *et al.*, Phys. Rev. C **37**, 587 (1988).

[36] P. Hoff and B. Fogelberg, Nucl. Phys. **A368**, 210 (1981).

[37] D. Zwarts, Comput. Phys. Commun. **38**, 365 (1985).

[38] G. Winter *et al.*, Phys. Rev. C **48**, 1010 (1993).

[39] G. Winter *et al.*, Phys. Rev. C **49**, 2427 (1994).

[40] X. Ji and B. H. Wildenthal, Phys. Rev. C **37**, 1256 (1988).

[41] R. Gross and A. Frenkel, Nucl. Phys. **A267**, 85 (1976).

[42] J. Blomqvist and L. Rydström, Phys. Scr. **31**, 31 (1985).

[43] G. de Angelis *et al.* (to be published).